Jurnal Teknologi

Full Paper

CHARACTERIZATION OF PHOTOCHEMICALLY INITIATED GOLD NANOPARTICLES SYNTHESIZED VIA INCOHERENT ULTRAVIOLET RADIATION

Jia-Cherng Chong[a], Siew-Ling Lee[b], Noriah Bidin[a*]

[a]Laser Center, Universiti Teknologi Malaysia, 81310 UTM Johor Bahru, Johor, Malaysia
[b]Ibnu Sina Institute for Fundamental Science Studies, Universiti Teknologi Malaysia, 81310 UTM Johor Bahru, Johor , Malaysia

*Corresponding author
noriah@utm.my

Article history
Received
10 February 2015
Received in revised form
10 November 2015
Accepted
12 November 2015

Graphical abstract

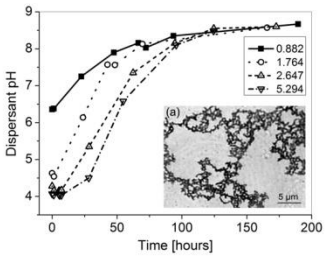

Abstract

A modified Turkevich pathway of synthesizing water suspended gold nanoparticles using incoherent ultraviolet radiation as photochemical reaction initiator produced broader absorbance band corresponding to localised surface plasmonresonsnce around 530 nm with average particle size separated into two distinct distributions from 5 nm to 100 nm depending on ultraviolet wavelength. Presence and dynamics of nanoparticle growth was observed with photon correlation spectroscopy where aged colloids produced submicron sized agglomerated particles. Post-synthesis colloidal pH shows gradual degradation of particle stability.

Keywords: Spherical AuNP; photochemical initiation; localised surface plasmon resonance (LSPR); photon correlation spectroscopy

Abstrak

Kami melaporkan kaedah penghasilan zarah nano emas melalui proses penurunan fotokimia sinaran ultraunggu. Berbanding dengan cara lazim iaitu tindakbalas Turkevich, terdapat bahawa proses penurunan fotokimia menghasilkan puncak yang lebih lebar dalams spektrum penyerapan disebabkan oleh kesan resonan permukaan plasmon setempat dalam lingkungan 530 nm. Didapati bahawa taburan saiz zarah terbahagi kepada dua berjulat antara 5 nm hingga 100 nm bergantung kepada tenaga foton. Dinamik proses pertumbuhan zarah nano telah dikenalpasti oleh alat photon correlation spectroscopy. Mendakan yang terdiri daripada zarah emas sebesar ratusan nanometer dapat dicerap melalui mikroskop cahaya.

Kata kunci: Zarah nano emas; tindakbalas fotokimia, localised surface plasmon resonance (LSPR); photon correlation spectroscopy

1.0 INTRODUCTION

The dimension and subsequent electronic properties of spherical gold nanoparticles (AuNP) gave rise to many potential optical applications, especially in the field of physical biochemistry. Lately, the emergence of applications such as novel cancer therapies[1-3], DNA markers[4], drug delivery[5-7] and biological contrast agenst[8-10] results a will of developing energy efficient synthesis methods for stable AuNPs. Citrate reduced AuNPs was developed by Turkevich using heat reflux to initiate reduction of gold ions and accelerate growth into nanosized particles where citrate ion itself behaves as both reducing and capping agent; Turkevich's method remain popular today for producing relatively monodisperseAuNPs rapidly. However, other methods

of triggering chemical reactions between the two reagents such as sonolysis[11,12], microwave induced heating[13-15] and ultraviolet photoinitiation[16-19] was found to produce AuNPs at lower energy requirement. The resultant colloidal characteristics from each synthesis pathway often depend heavily on parameters chosen by their investigators; as such, reports available in the literature makes the search for a detailed mechanism responsible for photoinitiatedAuNPs in citrate environment difficult.

To date, AuNPs produced via heat reflux has been extensively studied. By varying temperature, ionic ratio of reactants and stirring speed; particles with mean size from 10 nm to 100 nm can be produced. However, investigations in AuNPs produced via photochemical processes initiated by ultraviolet light so far provided limited knowledge on growth mechanism. In this report, we investigate time-resolved characteristics of AuNPs synthesized via both heat reflux and ultraviolet photoinitiation followed by remarks on its stability days after synthesis.

Table 1 Synthesis protocol for all AuNP samples where A and F are control for heat reflux and non-ultraviolet effects respectively.

Sample	$HAuCl_4$ Vol. [ml]	Na-citrate Vol. [µl]	Au : Cit ionic ratio	Synthesis method	Exposure [minutes]
A	30	300	0.882	Heat reflux[20]	5
B	30	150	1.764	UVA photoinitiation	10
C	30	150	1.764	UVC photoinitiation	10
D	30	120	2.206	UVA photoinitiation	15
E	30	120	2.206	UVC photoinitiation	15
F	30	300	0.882	UVC absence*	10
G	30	300	0.882	UVC photoinitiation	10
H	30	130	2.036	UVC photoinitiation	10
J	30	100	2.647	UVC photoinitiation	10
K	30	50	5.294	UVC photoinitiation	10

*Control created by complete filtering of UVC emissions, leaving visible component peaks from the light source for photoinitiation.

2.0 EXPERIMENTAL

All chemicals were purchased from Sigma Aldrich. Glassware involved in the synthesis was prewashed with aqua regia followed by rinsing with generous amount of ultrapure deionised water (18 MΩ SG systems) for removal of possible nucleation sites. A stock solution of 1.5 mM auric acid ($HAuCl_4 \bullet 3H_20$) and 1% w/v trisodium citrate ($Na_3C_6H_5O_7 \bullet 2H_20$) was prepared separately. A set of AuNP samples was synthesized by adding tri-sodium citrate into auric acid following protocol listed in Table 1.

Photochemically initiated AuNPs was exposed by two separate light sources; one transmitting singular 366 nm UVA radiation from 4 watts Wood's fluorescent lamp and another with multiple emission peaks from quartz enclosed mercury discharge tube with principal UVC emission at 253.7 nm. All photoinitiated samples were exposed through an aperture of 1 cm^2 at irradiance of 0.8 mW cm^{-2}. A control was created for UVC photoinitiated samples by complete filtering of shortwave peaks with 0.15 mm thick borosilicate glass.

The exposure time for sample A was recorded from the moment trisodium citrate was injected into boiling auric acid while it was rigorously stirred. Separate aliquots was extracted as colour of the solution change and cooled rapidly in ice bath to dampen reaction processes. The absorption spectrum of the aliquot was measured immediately by a fibre spectrophotometer (Avantes CUV-ALL-UV/VIS) with OceanOptics USB4000 and a tungsten-halogen light source. The final optical absorbance was recorded for sample A when its colour reached brilliant ruby red. After synthesis, acidity of all the samples was measured periodically by digital pH meter and they were kept for 8 days. The size distribution of the samples was measured via photon correlation spectroscopy with Malvern ZetasizerNano ZS.

3.0 RESULTS AND DISCUSSION

The standardized Turkevich synthesis is well known to produce relatively monodisperseAuNPs with diameter between 10 nm to 20 nm by adding trisodium citrate into boiling auric acid[20]. Upon heat and rigorous stirring after introduction of citrate ions, presence of AuNPs is indicated by the apparent change of solution colour slowly from clear light-yellow to grey followed rapidly into deep blue, purple and finally reaching brilliant ruby red. The change of colloidal colour is the direct consequence of Mie scattering characteristic to the size distribution of spherical AuNPs (Fig. 4) and it is reflected in the absorption spectra as development of a distinct peak around 510 nm to 550 nm. The absorbance profile corresponds to localized surface plasmon resonance (LSPR) of the electron gas in the nanoparticles, where the resonant frequency depends on size of the particles and wavelength-dependent refractive indices of both the material of the particle and its dispersant.

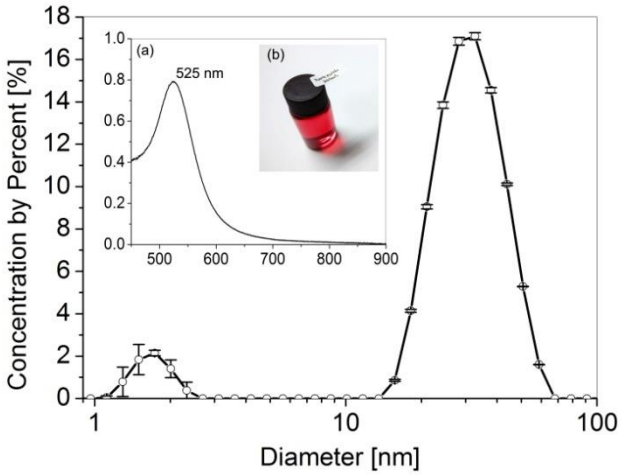

Figure 1 Particle size distribution of sample A with mean particle diameter of 32 nm. Inset (a)Absolute optical absorbance (vertical axis) against wavelength in nm (horizontal axis) shows LSPR peak at 525 nm. Inset (b**)**Visual appearance of sample A, 5 minutes after trisodium citrate was added to boiling auric acid.

The nucleation mechanism for AuNPs in citrate environment are generally accepted as stepwise reduction of Au (III) complex into Au (0)[20,21]: a fast ligand exchange with citrate anion to form an intermediate species followed by an equilibrium that provides a loop-closure allowing further slow, rate-determining step involving decarboxylation and final reduction of Au (I) species into neutral gold atoms.

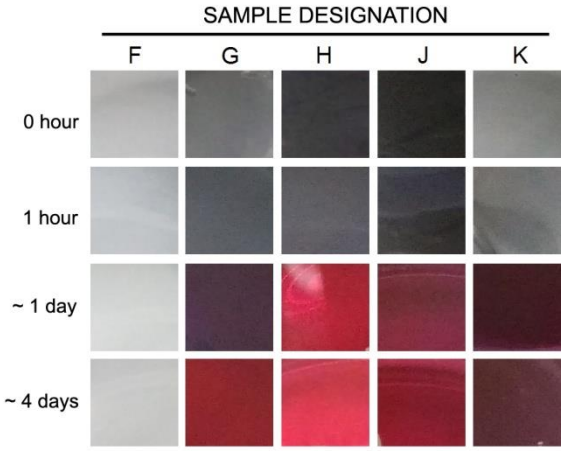

Figure 2 Colour cue of UVC photoinitiatedAuNP samples. Sample G, H, J and K have increasing Au :Cit ratio from 0.882 to 5.294 (ref. Table 1).

The rate-determining step depends on fast equilibrium established between $[AuCl_3(C_6H_5O_7)^{2-}]^-$ complex and its pentacoordinated intermediate created by deprotonation of alcohol group in $[AuCl^3(C^6H^5O^7)^{2-}]^-$ followed by coordination of remaining alcohol oxygen axially to Au (III). The pentacoordinated complex then disintegrates into Au (I) forming a multimolecular complex with decarboxyacetone molecules as part of the disintegrated components present in the solution. Increasing concentration of multimolecular complex ions finally causes disproportionation[22] among aurous species which shifts the equilibrium towards reduction of Au (I) into neutral gold atoms. In the absence of heat, it is found that ultraviolet photons are capable of photolysing Au (III) into bivalent Au (II) complex[23], subsequently producing Au (I) through mechanism mentioned earlier. OH radicals from direct ultraviolet photolysis of water shift the fast equilibrium to the pentacoordinated intermediate complex which results in higher concentration of Au (I). Ultraviolet photons may also decompose $AuCl^{4-}$ to $AuCl^{3-}$ producing Cl^- in solution that will accelerate the OH radical reaction causing an increase in Au (I) concentration.

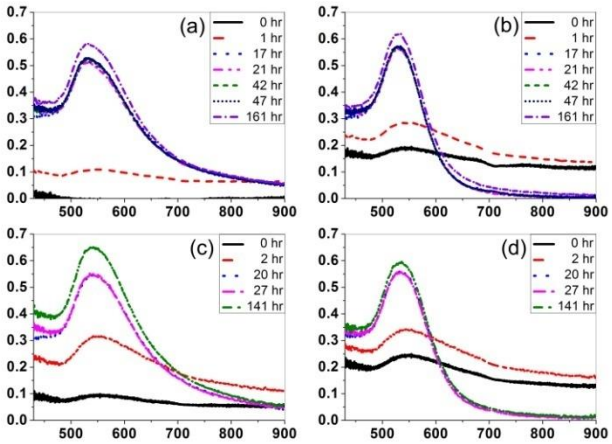

Figure 3(a), **(b)**, **(c)**, and **(d)** are absolute optical absorbance (vertical axes) against wavelength in nm (horizontal axes) for sample B, C, D, E respectively. Note significantly late development of LSPR peak around 530 nm in all four samples compared to heat refluxed AuNPs.

Despite increasing availability of Au (I) through photolytic processes, it will not be reduced to Au (0) as far as Au (III) species dominates the solution due to its strong negative redox potential[24], E^0 [Au (I)/Au (0)] at −1.4. The reduction method described by Turkevich uses heat to induce an energetic pathway for quick reduction of Au (III) into neutral Au (0) atoms. The increased random velocity of particles due to thermal excitation also results in faster development of LSPR peak in the absorption spectrum and also narrower particle size distribution compared to photochemically initiated AuNPs (Fig. 5). Since mobile ions in photoinitiated reactants are non-thermal, they depend on kinetics in molecular coordination at room temperature for the stepwise reduction to favour formation of Au (0) atoms; as a result, delay in appearance of LSPR bands (Fig. 3) in the optical absorbance is expected from photoinitiatedAuNPs.

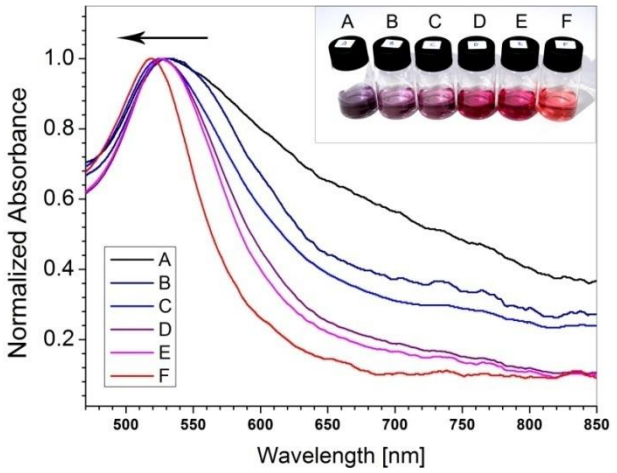

Figure 4 Normalized absorbance spectra shows LSPR peak development in sample A. The profile peak narrows towards 525 nm as sample colour changes from deep purple to bright ruby red. Inset Visual appearance of aliquots when size distribution and absorbance was measured during the reaction.

Normalizing optical absorbance (Fig. 4) obtained from aliquots of AuNPs synthesized via heat reflux shows LSPR band at different stages of agglomeration identified by their colour moments after citrate ions was introduced into hot auric acid. The colour change is reflected on the absorbance profile whereas the sample turns into brilliant red, absorbance peak blue-shifted. The same order of evolution in colour and absorbance was observed in all photoinitiated samples but at a much slower rate. Comparing heat and ultraviolet initiated AuNPs, thermally reduced AuNPs exhibit narrowest peak-profile in both optical absorbance and size distribution almost immediately after trisodium citrate was introduced. The rate of reaction considered negligible after 5 minutes of heating when changes in optical absorbance has stopped; the terminal absorbance profile is identified as the peak blue-shifted towards 520 nm. In contrast, ultraviolet initiated samples starts to show changes in its optical absorbance hours after the reactants were exposed to ultraviolet radiation. UVC initiated AuNPs (Fig. 3(b) and 3(d)) generally shows narrower and faster development of LSPR peak compared to UVA initiated samples (Fig. 3(a) and 3(c)).

Following numerical solutions to calculate extinction coefficient of monodisperseAuNPs due to Mie scattering, the narrowing and blue-shift of absorbance bandwidth around 550 nm towards 525 nm implies increasing concentration of smaller particles within the sample; this counter-intuitive change in particle size distribution was not fully understood until new insights in nucleation mechanism proposed by Pong *et. al.* suggests the particles formed an intermediate network of gold nanorods[25] throughout the sample when it is still in the purplish-blue stage before fragmenting into smaller spherical AuNPs due to electrostatic repulsion and stearic hindrance of citrate ions adhered to certain crystalline facets of gold nanocrystals as it grows.

The size distribution of the AuNP samples measured via photon correlation spectroscopy compliments the optical absorbance spectra. The difference of time required to develop an LSPR peak between the photoinitiated samples suggest the rate of agglomeration is affected by specific quantisation rather than intensity of radiation (Fig. 3). This effect might be contributed to photolysis of water which occurs when it is exposed to UVC rather than UVA radiation. OH radicals liberated from photolysed water molecule shift the equilibria of aureous species favouring production of Au (I), thus increasing neutral gold atoms available for nanoparticle growth.

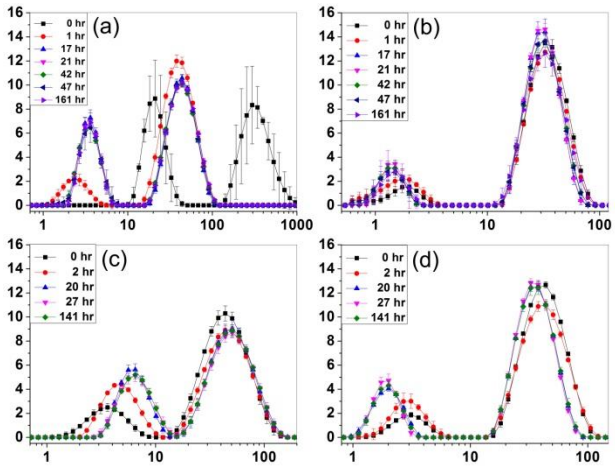

Figure 5 (a), **(b)**, **(c)** and **(d)** correspond to percentile of particles (vertical axes) with its diameter in nm (horizontal axes) for sample B, C, D, E respectively. Note broader size distribution for sample with higher gold to citrate ratio (c) and (d) and samples initialized by UVA emissions.

The ratio of reactant ions affects the rate and final state of agglomeration greatly. It was found that UVC photoinitiated samples at gold to citrate ratio of 2.01 produced fastest change of colour from grey to red in less than 24 hours (Fig. 2) while samples prepared using lesser concentration of citrate ions generally result in larger particle size distribution (Fig. 5 (c), (d)). This is in accordance with UVA initiated AuNPs reported by Kimling*et. al.* using similar methods[19] which resulted wide size distribution ranging from 30 nm to 70 nm in diameter. If the ionic ratio exceeds 2.65, the state of agglomeration changes slowly, reaching ruby red appearance days after photoinitiation. Neither colour change nor a distinct LSPR band was observed in sample F, which was exposed only to visible light and near infrared radiation emitted from mercury vapour discharge; the absence of an absorbance peak indicates the photoinitiation process depends on ultraviolet rather than visible light.

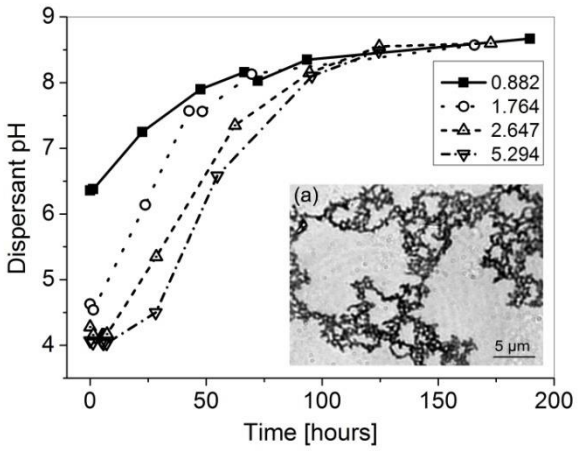

Figure 6 pH values of UVC photoinitiatedAuNPs (sample G, H, J and K) indicating agglomeration of particles as the sample ages. Legend indicates Au :Cit ratio. Inset (a) 1000X bright-field micrograph of sample K, 8 days after initiation.

An unstable colloidal system typically leads to agglomeration of the nanoparticles over extended period of time if zeta potential of the double layer on the nanoparticles created by electrostatic interactions of adsorbed citrate branches and its surrounding counter ions is weakened by changes in dispersant pH. Thus, the dispersant's pH qualitatively describes the stability of the AuNPs by measuring concentration of free H^+ ions. Immediately following the introduction of trisodium citrate, the colloidal pH raised from initial H^+ concentration to values dictated by the equilibrium established between the citrate ions and all intermediate aurous complexes. As reduction and nucleation was triggered by any initiation methods; subsequent stepwise reduction of aureous species changes the equilibria which result increase in pH value as a consequence of increasing ionic layer. The particles eventually grow up to submicron sizes (Fig. 6 (a)) and sediments were observed on the bottom of the container days after the samples were synthesized. In all UVC initiated AuNPs, their pH values plateau towards 8.5 after five days of aging. The cessation of change in pH is reflected by increase and broadening of LSPR peak in optical absorbance indicating presence of larger particles.

4.0 CONCLUSION

Photochemical initialization of citrate reduced AuNPs by both 253.7 nm and 366 nm produced relatively monodisperse particles having mean peak diameter of 32.7 nm and 43.8 nm respectively. The size distributions of UVC photoinitialized samples are close in dimension with AuNPs prepared via heat reflux. The optical absorbance shows blue-shifting and bandwidth narrowing identical to photochemically initiated AuNPs at a much slower rate under same irradiance. UVC initiated samples exhibit faster development of LSPR peak towards 520 nm compared to UVA photoinitiation with generally narrower peak profile. For 8 days post UVC photoinitiation, the samples shows gradual increase in pH towards 8.5. The degradation of colloidal stability was observed by increasing and broadening LSPR peak in the absorption spectra.

Acknowledgement

This research was supported by Malaysian higher education MOHE through FRGS vote 4F543 and MyBrain scholarship for the first author to pursue his PhD program in UTM.

References

[1] C. S. Regiya, Jatish Kumar, V. Raji, M. Vibin, A. Annie. 2012. Selective Photothermal Efficiency Of Citrate Capped Gold Nanoparticles For Destruction Of Cancer Cells. *Pharmacological Research*. 65: 261-269.

[2] J.L. Li, Min Gu. 2010. Gold-Nanoparticle-Enhanced Cancer Photothermal Therapy. *IEEE Journal on Selected Topics in Quantum Electronics*. 16(4): 989-996.

[3] X. H. Huang, Prashant K. Jain. I. H. El-Sayed, M. A. El-Sayed. 2008. Plasmonic Photothermal Therapy (PPTT) Using Gold Nanoparticles. *Lasers Med. Sci.* 23: 217-228.

[4] Y. P. Liu, W. Meyer-Zaika, S. Franzka, G. Schmid, M. Tsoli, H. Kuhn. 2003. Gold - Cluster Degradation by the Transition of B - DNA into A - DNA and the Formation of Nanowires Angew. *Chem. Int. Ed.* 42: 2853-2857.

[5] J. H. Park, G. Maltzahn, L. L. Ong, A. Centrone. T. A. Hatton, E. Ruoslahti, S. N. Bhatia, M. J. Sailor. 2010. Cooperative Nanoparticles for Tumor Detection and Photothermally Triggered Drug Delivery. *Adv. Mater.* 22: 880-885.

[6] A. G. Tkachenko, H. Xie, Y. L. Liu, D. Coleman, J. Ryan, W. R. Glomm, M. K. Shipton, S. Franzen, D. L. Feldheim. 2004. Cellular Trajectories of Peptide-modified Gold Particle Complexes: Comparison of Nuclear Localization Signals and Peptide Transduction Domains. *Bioconjugate Chem.* 15: 482-490.

[7] M. Thomas, A. M. Klibanov. 2003, Conjugation to Gold Nanoparticles Enhances Polyethylenimine's Transfer of Plasmid DNA into Mammalian Cells. *Proc. Nat. Aca. Sci*. 100(16): 9138-9143.

[8] G. Maltzahn, A. Centrone, J. H. Park, R. Ramanathan, M. J. Sailor, T. A. Hatton, S. N. Bhatia. 2009. SERS - coded Gold Nanorods as a Multifunctional Platform for Densely Multiplexed Near - infrared Imaging and Photothermal Heating. *Adv. Mater.* 21: 3175-3180.

[9] H. J. Parab, H. M. Chen, T. C. Lai, J. H. Huang, P. H. Chen, R. S. Liu, M. Hsiao, C. H. Chen, D. P. Tsai, Y. K. Hwu. 2009. Biosensing, Cytotoxicity, and Cellular Uptake Studies of Surface-modified Gold Nanorods. J. *Phys. Chem. C*. 113(18): 1574-1578.

[10] C. J. Murphy, A. M. Gole, J. W. Stone, P. N. Sisco, A. M. Alkilany, E. C. Goldsmith, S. C. Baxter. 2008. Gold Nanoparticles in Biology: Beyond Toxicity to Cellular Imaging. *Acc. Chem. Research*. 41(12): 1721-1730.

[11] J. E. Park, M. Atobe, F. Fuchigami. 2006. Sonochemical Synthesis of Conducting Polymer–metal Nanoparticles Nanocomposite. *Ultrason. Sonochem.* 13: 237-241.

[12] K. Okitsu, M. Ashokkumar, F. Grieser. 2005. Sonochemical Synthesis of Gold Nanoparticles: Effects of Ultrasound Frequency. *J. Phys. Chem. B.*, 109: 20673-20675.

[13] S. Kundu, K. Wang, H. Liang. 2009. Size-controlled Synthesis and Self-assembly of Silver Nanoparticles within a Minute using Microwave Irradiation. *J. Phys. Chem. C*. 113(13): 5157-5163.
[14] J. Gu, W. Fan, A. Shimojima, T. Okubo. 2008. Microwave-Induced Synthesis of Highly Dispersed Gold Nanoparticles Within the Pore Channels of Mesoporous Silica. *J. Solid State Chem.* 181(4): 957-963.
[15] F. Liua, Y. Chang, F. Koa, T. Chu. 2004. Microwave rapid Heating for The Synthesis of Gold Nanorods. *Mater. Lett.* 58(3): 373-377.
[16] S. Yang, T. Zhang, L. Zhang, S. Wang, Z. Yang, B. Ding. 2007. Continuous Synthesis of Gold Nanoparticles and Nanoplates with Controlled Size and Shape Under UV Irradiation. *Colloids Surf. A*. 296: 37-44.
[17] M. Meyre, M. Treguer-Delapierre, C. Faure. 2008. Radiation-induced Synthesis of Gold Nanoparticles within Lamellar Phases. Formation of Aligned Colloidal Gold by Radiolysis. *Langmuir*. 24(9): 4421-4425.
[18] T. K. Sau, A. Pal, N. R. Jana, Z. L. Wang, T. Pal. 2001. Seed-mediated Successive Growth of Gold Particles Accomplished by UV Irradiation: A Photochemical Approach for Size-controlled Synthesis. *J. Nanopart. Res.* 3(4): 257-261.
[19] J. Kimling, M. Maier, B. Okenve, V. Kotaidis, H. Ballot, A. Plech, 2006. Turkevich Method for Gold Nanoparticle Synthesis Revisited. *J. Phys. Chem. B* 110, 15700-157707.
[20] J. Turkevich, P. C. Stevenson, J. Hiller. 1951. A Study of the Nucleation and Growth Processes in the Synthesis of Colloidal Gold. *Discuss. Faraday Soc.* 11: 55-75.
[21] Rodrígez-Gonzalez, B. Mulvaney, P. Liz-Marzán, L. M. Z. 2007. Small Gold Nanoparticles Synthesized with Sodium Citrate and Heavy water: Insights into the Reaction Mechanism. *Phys. Chem.* 221: 415-426.
[22] X. Wu, P. L. Redmond, H. Liu, Y. Chen, M. Steigerwald, L. J. Brus. 2008. Photovoltage Mechanism for Room Light Conversion of Citrate Stabilized Silver Nanocrystal Seeds to Large Nanoprisms. *Am. Chem. Soc.*130: 9500-9506.
[23] M. Kaushik, Z. L. Wang, P. Tarasanka, 2001. Seed-mediated Successive Growth of Gold Particles Accomplished By UV Irradiation: A Photochemical Approach For Size-controlled Synthesis. *J. Photochemistry and Photobiology A: Chem*, 140: 75-80.
[24] B. Cercek, M. Ebert, A.J. Swallow. 1966. Novel Valence States of Thallium as Studied by Pulse Radiolysis. *J. Chem. Soc. A*. 612-615.
[25] B. K. Pong, H. I. Elim, J. X. Chong, W. Ji, B. L. Trout, J. Y. Lee. 2007. New Insights on the Nanoparticle Growth Mechanism in The Citrate Reduction of Gold(III) salt: Formation of the Au Nanowire Intermediate and Its Nonlinear Optical Properties. *J. Phys. Chem. C*. 111: 6281-6287.